Drug Design, Development and Therapy

Dovepress

open access to scientific and medical research

Open Access Full Text Article

ORIGINAL RESEARCH

Synthesis and characterization of a glycine-modified heptamethine indocyanine dye for in vivo cancer-targeted near-infrared imaging

This article was published in the following Dove Press journal:
Drug Design, Development and Therapy
9 September 2014
Number of times this article has been viewed

Tao Liu[1]
Shenglin Luo[1]
Yang Wang[1]
Xu Tan[1]
Qingrong Qi[2]
Chunmeng Shi[1]

[1]Institute of Combined Injury, State Key Laboratory of Trauma, Burns and Combined Injury, Chongqing Engineering Research Center for Nanomedicine, College of Preventive Medicine, Third Military Medical University, Chongqing, People's Republic of China; [2]Key Laboratory of Drug-Targeting and Drug-Delivery Systems of the Ministry of Education, Department of Medicinal Chemistry, West China School of Pharmacy, Sichuan University, Chengdu, People's Republic of China

Abstract: Near-infrared (NIR) fluorescent sensors have emerged as promising molecular tools for cancer imaging and detection in living systems. However, cancer NIR fluorescent sensors are very challenging to develop because they are required to exhibit good specificity and low toxicity as an eligible contrast agent. Here, we describe the synthesis of a new heptamethine indocyanine dye (NIR-27) modified with a glycine at the end of each N-alkyl side chain, and its biological characterization for in vivo cancer-targeted NIR imaging. In addition to its high specificity, NIR-27 also shows lower cytotoxicity than indocyanine green, a nonspecific NIR probe widely used in clinic. These characteristics suggest that NIR-27 is a promising prospect as a new NIR fluorescent sensor for sensitive cancer detection.

Keywords: near-infrared (NIR), heptamethine dye, cancer-targeted imaging

Introduction

Noninvasive imaging with light photons represents an intriguing avenue to explore for cancer detection and diagnosis.[1] In particular, much attention has been paid to near-infrared (NIR) fluorescence imaging within the wavelength range of 700–900 nm due to its low absorption and autofluorescence from organisms and tissues in the NIR spectral range, rendering minimal background interference, deep tissue penetration, and high sensitivity for cancer imaging.[2,3] The heart of NIR imaging lies in the development of fulfilling fluorochromes, which must have a high molar absorption coefficient for intense fluorescence, good biocompatibility with low toxicity, and sufficient stability and water solubility in the complex biological environment. Most importantly, a qualified cancer NIR sensor should have high specificity for cancer-selective detection. However, to the best of our knowledge, none of the NIR probes meet all the requirements mentioned above. For example, indocyanine green (ICG), the only clinically approved NIR heptamethine indocyanine dye, has been used for over 50 years with non-specificity.[4] Moreover, there have been reports of few side effects due to administration of ICG.[5–7] There is an urgent need to develop specific and low-toxic NIR sensors for cancer-sensitive imaging.

In order to achieve cancer-targeted NIR imaging, a number of researchers have designed and synthesized various ICG derivatives, which are modified with some functional groups available for further conjugation of cancer-specific ligands, such as folate,[8,9] cyclic RGD peptide (cRGD, a target for the αvβ3 integrin)[10,11] and cancer-targeting antibodies.[12,13] Despite the fact that the conjugation strategies described above demonstrate some efficacy, the specificity for drug delivery, the potency of cancer therapeutics, and the potential for clinic application still remain unsatisfactory.[14] On

Correspondence: Chunmeng Shi
Institute of Combined Injury,
Third Military Medical University,
30 Gaotanyan Road, Chongqing 400038,
People's Republic of China
Email shicm@sina.com

© 2014 Liu et al. This work is published by Dove Medical Press Limited, and licensed under Creative Commons Attribution – Non Commercial (unported, v3.0) License. The full terms of the License are available at http://creativecommons.org/licenses/by-nc/3.0/. Non-commercial uses of the work are permitted without any further permission from Dove Medical Press Limited, provided the work is properly attributed. Permissions beyond the scope of the License are administered by Dove Medical Press Limited. Information on how to request permission may be found at: http://www.dovepress.com/permissions.php

the one hand, chemical conjugation may alter the functional activities of targeting ligands, imaging agents, or therapeutic agents.[15] On the other hand, conjugation strategy means additional synthetic steps and costs, more convoluted behavior and effects in vivo, and also greater regulatory hurdles in applying for clinic trials and extensive applications.[16]

Recently, we reported on two heptamethine NIR cyanine dyes (IR-780 and IR-808) characterized with tumor-targeted accumulation without the requirement of chemical conjugation to tumor-specific ligands.[17–20] Their tumor-targeted abilities have been verified in a broad spectrum of tumor cell lines and tumor xenografts, providing a new strategy and promising prospects for simultaneous cancer targeting and imaging. However, both of them exhibit high lipophilicity and cytotoxicity when a high dosage is used, inevitably impeding their clinical adoption. Amino acids are a water-soluble group and exist extensively in living creatures as the essential nutrients for cell growth. In particular, amino acids have recently been explored as a tumor-targeted moiety for cancer targeting and imaging.[21] Based on our previous findings, we herein develop a new glycine-modified heptamethine cyanine dye (NIR-27) to obtain a water-soluble and good biocompatible NIR probe with high tumor specificity.

Materials and methods

Apparatus and materials

Apparatus

Nuclear magnetic resonance spectra (^{1}H NMR and ^{13}C NMR) and high-resolution mass spectra (HRMS) were used to structural characterization. ^{1}H NMR and ^{13}C NMR were recorded with a nuclear magnetic resonance spectrometer (600MHz NMR; Varian Corporation, Palo Alto, CA, USA) in either $CDCl_3$ or CD_3OD by using trimethylchlorosilane as an internal standard. The NMR signals were described with symbols s for singlet, d for doublet, t for triplet, m for multiplet. Chemical shifts (δ) were reported in ppm and coupling constants (*J*), are reported in hertz (Hz). HRMS was recorded with a Bruker BioTOFIIIQ system (Bruker Corporation, Billerica, MA, USA). Fluorescence spectroscopy was determined by using a Varian fluorescence spectrophotometer (Cary Edlipse; Varian Corporation). NIR absorption spectroscopy was determined by using a Shimadzu Spectrophotometer (UV-3600; Shimadzu Corporation, Kyoto, Japan). NIR imaging was performed by using a Kodak In-Vivo FX Professional Imaging System (Rochester, NY, USA).

Materials

Glycine (98%), 6-bromohexanoic acid (98%) and 2,3,3-trimethyl-3*H* indole (98%) were purchased from ACROS (Beijing, People's Republic of China). Rhodamine123 was purchased from Sigma-Aldrich Co (St Louis, MO, USA). Thin layer chromatography was used to monitor chemical reactions with GF254 silica gel plates. Products were purified with silica gel flash chromatography. Arium pro ultrapure water (18.2 MΩ cm; Sartorius Stedim Biotech GmbH, Goettingen, Germany) was used throughout the analytical experiments.

Synthesis and characterization of NIR-27

Methyl 2-(6-bromohexylamino)-2-oxoacetate (compound 4)

According to a reported protocol[22] for preparing its analogues, compound 4 was synthesized to give 7.70 g of pure production with a yield of 60%. Melting point (Mp): 51°C–52°C ^{1}H NMR (400 MHz, $CDCl_3$) δ: 5.99(s, 1H), 4.06 (d, *J*=5.1 Hz, 2H), 3.77 (s, 3H), 3.41 (t, *J*=6.7 Hz, 2H), 2.27 (t, *J*=7.5 Hz, 2H), 1.86 (m, 2H), 1.69 (m, 2H), 1.49 (m, 2H).

2-(6-bromohexanamido) acetic acid (compound 5)

A mixture solution of tetrahydrofuran/H_2O (120 mL: 30 mL) was added to lithium hydroxide monohydrate (1.02 g, 0.02 mol). After the stirred solution was cooled to 0°C, compound 4 (6.0 g, 0.02 mol) was added, then stirred for another 3 hours. The reaction mixture was neutralized with 5% diluted hydrochloric acid and extracted with ethyl acetate (3×50 mL), The combined extracts were washed with brine (3×50 mL), dried over anhydrous Na_2SO_4, and removed under reduced pressure to yield a faint yellow oil. Recrystallization from ether yielded a white solid of pure product (4.14 g, 75%). Mp: 76°C–78°C; ^{1}H NMR (400 MHz, $CDCl_3$) δ: 8.56 (s, 1H), 6.33 (s, 1H), 4.08 (d, 2H), 3.41 (t, 2H), 2.31 (t, 2H), 1.86 (m, 2H), 1.57 (m, 2H), 1.49 (m, 2H).

1-(6-(carboxymethylamino)-6-oxohexyl)-2,3,3-trimethyl-3H-indolium bromide (compound 7)

According to a reported protocol[23] with some modification, compound **7** was synthesized. Briefly, a mixture of 2,2,3-trimethyl-3H-indolenine (3.84, 0.02 mol), compound 5 (7.70, 0.03 mol), and toluene (30 mL) was heated at 110°C under argon in a 50 mL flask for 12 hours. The reaction mixture was cooled to room temperature, and the toluene was evaporated under reduced pressure to yield a reddish oil (5.08, 50%). The crude product was used for synthesis of NIR-27 without further purification.

Synthesis of NIR-27

In a 100 mL round flask, 2-chloro-1-formyl-3-hydroxymethylene cyclohexene (0.67, 3.87 mmol), quaternary

salt compound **7** (5.08 g, 7.75 mmol), and sodium acetate (0.66 g, 7.75 mmol) were mixed in 40 mL of absolute ethanol under argon and heated at 70°C for 1 hour. After completion of the reaction, the ethanol was evaporated under reduced pressure and the green residue was dissolved in a small amount of dichloromethane. The crude product was precipitated from dichloromethane by the addition of a triple amount of ether. The pure product of NIR-27 (0.51 mg) was obtained by silica gel column chromatography (eluent solvent; chloroform: methanol 5:1), with a yield of 15%. Its purity was characterized with high-performance liquid chromatography (98.9%). ^{1}H NMR (600 MHz, CD_3OD) δ: 8.420 (d, 2H), 7.511 (d, 2H), 7.412 (d, 2H), 7.339 (d, 2H), 7.283 (d, 2H), 6.290 (d, 2H), 4.180 (s, 4H), 3.719 (s, 4H), 3.299 (s, 4H), 2.721 (s, 4H), 2.262 (s, 4H), 1.956 (s, 2H), 1.853 (s, 4H), 1.719 (s, 4H), 1.491 (s, 4H); ^{13}C NMR (300 MHz, CD_3OD): 176.83, 175.35, 174.14, 150.98, 145.41, 143.58, 142.57, 129.94, 128.02, 126.55, 123.51, 112.36, 102.40, 50.62, 48.36, 45.08, 44.51, 36.61, 28.31, 28.15, 27.38, 26.35, 22.13. ESI-HRMS: m/z Calcd 797.4039 $[M-Br]^+$, found 797.3896 $[M-Br]^+$.

Optical properties

Optical properties of NIR-27 in methanol, serum, and phosphate-buffered saline (PBS) were determined by the methods reported previously.[24,25] To evaluate stability in serum, 10 μM NIR-27 was incubated in 100% fetal bovine serum at 37°C for 96 hours. Fluorescence intensities were detected in black 96-well plates by a Biotek Synergy H4 Hybrid Microplate Reader (740 nm excitation, 800 nm emission with 9 nm slit width; BioTek US, Winooski, VT, USA).

Cell lines and cell culture

Human lung cancer cells (A549), human bronchial epithelial cells (HBE), human leukemia cells (HL-60), and green fluorescent protein (GFP)-labelled HL-60 (HL-60 cells with stable GFP expression) were maintained in Roswell Park Memorial Institute 1640 culture media. Gastric cancer cells (MKN-45), human hepatoma cells (HepG2), and human hepatocyte cells (LO2) were cultured in Dulbecco's Modified Eagle's medium culture media. All of the above culture media were supplied with 10% fetal bovine serum, 100 U/mL penicillin, and 100 μg/mL streptomycin. All of the cells were incubated at 37°C with 5% CO_2. At 70% confluence, cells were split with 1:3 ratios.

Tumor xenograft models

To establish MKN-45, A549, and GFP-labelled HL-60 tumor xenografts, male athymic BALB/c nude mice (4–6 weeks old) were injected subcutaneously in the left or right flank with 5×10^6 MKN-45, A549, or GFP-labelled HL-60 cells suspended in 200 μL PBS. All the experiments were done in triplicate. The nude mice were purchased from the laboratory animal center of the Third Military Medical University. In the process of operation, the animal protocols strictly complied with the "Animal Care and Use Committee Guidelines of the Third Military Medical University".

In vivo and ex vivo optical imaging

After injection with NIR-27 dye, whole body optical imaging was taken using a Kodak In-Vivo FX Professional Imaging System at different time points. All the settings were applied as described previously.[17] The nude mice bearing MKN-45, A549, or GFP-labelled HL-60 tumor xenografts were used and the dosage of NIR-27 dye was 0.3 mg/kg. To evaluate the dynamic dye accumulation and retention in tumors, the contrast index values were calculated as described in the literature.[26] In order to calculate the fluorescent intensity, the Kodak MI software 5.0.1 was used. After the tumor-bearing nude mice were sacrificed, dissected organs and tumors were obtained for fluorescent imaging.

Biodistribution of NIR-27 in normal mice

After intravenous injection of NIR-27 at a dose of 0.3 mg/kg, the normal mice were sacrificed at 0, 24, 48, and 96 hours (n=3 at each time point), and the dissected organs were subjected to NIR imaging by a Kodak In-Vivo FX Professional Imaging System to identify tissue distribution of NIR-27.[17,24]

Subcellular localization of NIR-27

To observe the subcellular localization of NIR-27 in cancer cells, a mitochondrial specific tracking dye, rhodamine 123, was co-stained with NIR-27 and imaged with confocal laser scanning fluorescence microscopy. Briefly, HL-60, MKN-45, and A549 cells were seeded into a 35 mm petri dish at a density of 2×10^4 cells/well, respectively. After incubation for 24 hours, the cells were incubated with NIR-27 at a concentration of 50 μM in serum-free medium for 30 minutes at 37°C, followed by the addition of 10 μM rhodamine 123 for an additional 10 minutes. Finally, nuclei were stained with Hoechst stains (Sanofi-Aventis, Bridgewater, NJ, USA).

Cytotoxicity assay

The cytotoxicity of NIR-27 and ICG were performed on A549, HBE, HepG2, and LO2 cells with the cell counting

kit-8 (CCK-8) assay as described previously.[27] The CCK-8 was purchased from Dojindo Laboratories (Kumamoto, Japan), and ICG from Sigma-Aldrich Co. In brief, the cells were cultured at a density of approximate 3,000 cells per well in a 96-well plate at 37°C with 5% CO_2 for 24 hours. Then cells were treated with the various formulations at a range of concentrations for 48 hours. After this incubation period, cell viability was monitored by using the CCK-8 assay according to the manufacturer's instructions. All the experiments were done in sextuplicate.

Acute toxicity of NIR-27 in rats

To assess the acute toxicity of NIR-27 in vivo, nine healthy male rats (100–130 g) were randomly divided into three groups: control group, 3 mg/kg NIR-27 group, and 30 mg/kg NIR-27 group. The control rats were injected with the 300 μL of saline via the tail vein. In the treated animals, deviations in normal behavior, coat condition, feces, movements, and mortality were monitored daily, and body weight changes were recorded within 7 days. All rats were sacrificed at the seventh day after administration of NIR-27, and the blood samples were collected to examine for blood cell counts and biochemical indicators. All tissues were fixed by 4% formaldehyde, made into paraffin sections, and hematoxylin and eosin staining was carried out for histological examination.

Results and discussion

As shown in Figure 1, synthesis of NIR-27 was started with 6-bromine hexanoic acid as the initial material, and completed in five steps that could be scaled up to gram-level production. NIR-27 was easily purified by column chromatography. The structure of NIR-27 was characterized using ^{1}H NMR, ^{13}C NMR, and HRMS (see Figures S1–S3). In contrast to IR-780 and IR-808, NIR-27 can be easily dissolved in water. The absorption and fluorescence spectra of NIR-27 were investigated in methanol, serum, and PBS (Figure 2A and B). The absorption and emission peak of NIR-27 in different media (methanol, serum, and PBS) lie in the NIR region (700–900 nm). The molar absorption coefficient (ε, mol^{-1} cm^{-1} L) in methanol was calculated up to 300,000 mol^{-1} cm^{-1} L. The emission intensity of NIR-27 and ICG in serum was much higher than in PBS (Figure 2C). The total fluorescence intensity of NIR-27 and ICG in serum was maintained at a stable level for 90 minutes, which indicates that NIR-27 and ICG are quite stable in serum (Figure 2D), suggesting that they have promising potential as an NIR probe in biomedical imaging.

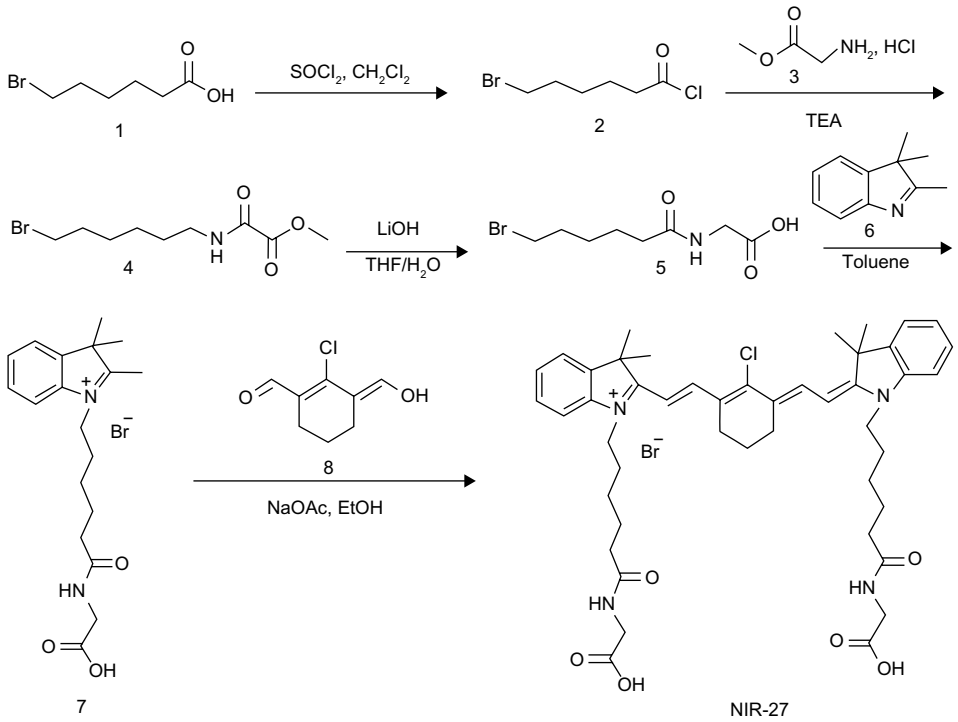

Figure 1 Synthetic route of NIR-27.
Abbreviations: NIR-27, heptamethine indocyanine dye; TEA, triethylamine; EtOH, ethanol; THF, tetrahydrofuran; NaOAc, sodium acetate.

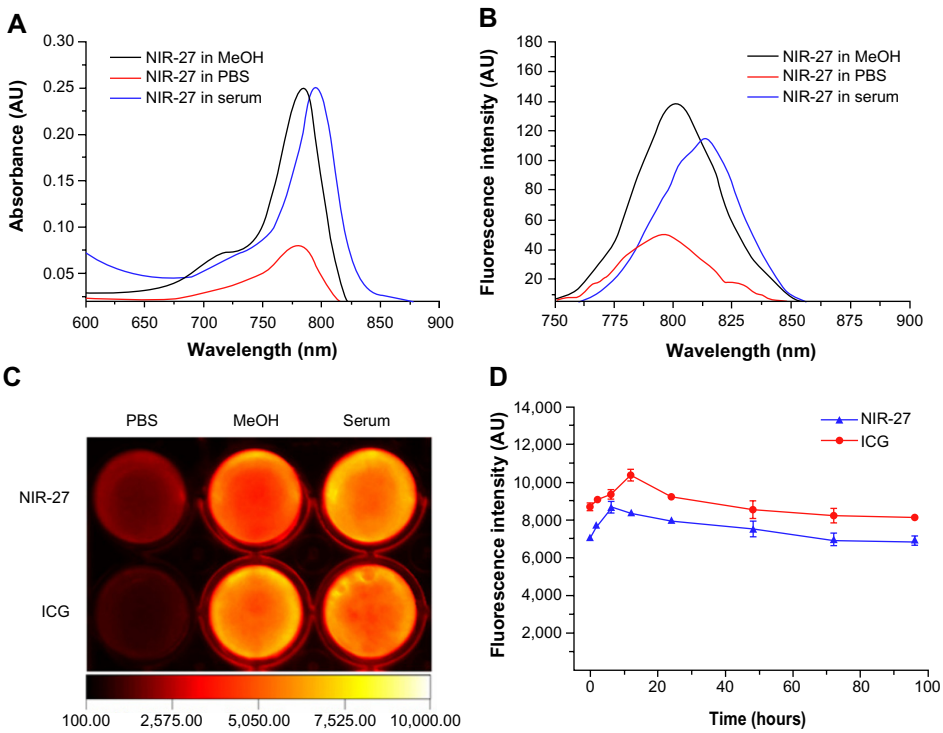

Figure 2 Optical properties of NIR-27.
Notes: (**A** and **B**): The absorption and emission spectra of NIR-27 (2 μM) in methanol (MeOH), PBS, and 100% FBS (serum). (**C**) Fluorescent image of NIR-27 and ICG (10 μM) in PBS, methanol, and 100% FBS. (**D**) Fluorescence stability of NIR-27 and ICG (10 μM) in 100% FBS at 37°C for 96 hours. Each valid point and vertical bar shows mean ± SD (n=3).
Abbreviations: FBS, fetal bovine serum; ICG, indocyanine green; NIR-27, heptamethine indocyanine dye; PBS, phosphate-buffered saline; SD, standard deviation.

Multiple human tumor xenograft models were used to investigate the tumor preferential accumulation of NIR-27 in vivo. Athymic BALB/c nude mice with human MKN-45, A549, and GFP-labelled HL-60 tumor xenografts in the subcutaneous spaces were established and subjected to NIR imaging after a single dose administration of NIR-27 at 0.3 mg/kg through intravenous injection. Figure 3A shows that NIR florescence signals associated with the implanted MKN-45, A549, (see Figure S4) and GFP-labelled HL-60 tumor xenograft sites can be clearly visualized with low background interfering signals after injection with NIR-27. Furthermore, fluorescence of NIR and GFP can be observed to be co-localized in the area of the tumor. The NIR fluorescence signals of the dissected organs further confirmed the cancer-targeting ability of NIR-27 in vivo (Figure 3B). Moreover, the cytosol accumulation of NIR-27 in GFP-labelled HL-60 tumor cells was identified by histopathologic analysis of the tumor specimens (Figure 3D). In addition, we also observed that the fluorescent signals continued for 14 days after a single injection of NIR-27 in the athymic nude mice bearing HL-60 tumor xenograft (see Figure S5). These results suggest NIR-27 can not only be preferentially accumulated in multiple tumors, but also maintain stable retention for a long time. The subcellular localization of the dye in tumor cells further showed that NIR-27 exclusively accumulated in the mitochondria of a variety of tumor cells by co-localization with mitochondrial tracker rhodamine 123 (Figure 3C). Therefore, we consider this dye as a potential diagnostic agent for sensitive and noninvasive cancer detection.

The cytotoxicity of NIR-27, compared with ICG, was evaluated after incubation with the A549, HBE, HepG2, and LO2 cells at different concentrations for 48 hours (Figure 4A). Then the cell viabilities were assessed using the colorimetric CCK-8. As shown in Figure 4A, no significant decrease in viability was observed in either of the two dyes, proving that NIR-27 and ICG did not exhibit obvious growth inhibition effects on the four kinds of cells we tested. On HBE and LO2 cells, the cell viability declined as the concentration of ICG increased, suggesting that ICG more easily killed some normal human cells than NIR-27 in the higher concentrations. The high viability values determined from the cells suggest that even a high concentration of 120 μM NIR-27 does not generate obvious cytotoxicity. Such a concentration is much higher than the highest concentration used for cell staining and NIR imaging. In further in vivo studies, the acute toxicity of the NIR-27 probes in rats was assessed. We chose doses of 10- and 100-fold of the imaging dose to observe the acute

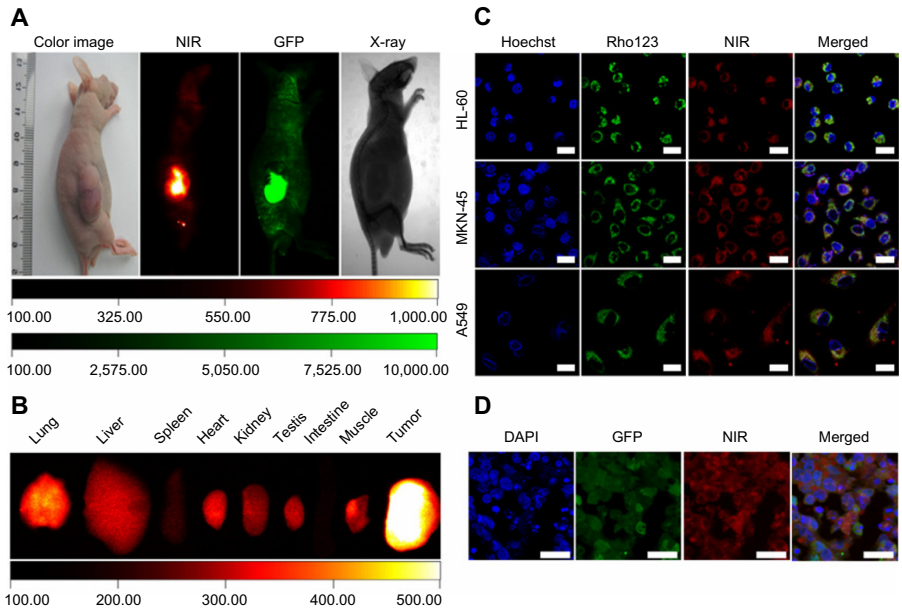

Figure 3 The preferential accumulation of NIR-27 in tumor xenografts.

Notes: (**A**) Images of the preferential accumulation of NIR-27 in athymic nude mice bearing pre-established GFP-labelled HL-60 tumor xenografts were shown. The mice were successively subjected to NIR imaging, GFP imaging, and X-ray imaging with the Kodak in vivo imaging system FX Pro after administration of NIR-27 at a dose of 0.3 mg/kg (n=3). The point-like accumulation far from the main tumor were general skin abrasions in the nude mouse. (**B**) The fluorescent intensity of dissected organs further confirmed the preferential accumulation of NIR-27 in tumors. (**C**) Subcellular localization of NIR-27. Co-localization of NIR-27 with mitochondrial-specific tracker, rhodamine 123, in cultured HL-60, MKN-45, and A549 tumor cells as imaged by confocal microscope. (**D**) Histopathologic analysis of GFP-labelled HL-60 tumor specimens by confocal microscope. Nuclei were stained with DAPI (blue). The bars in (**C** and **D**) indicate 20 μm.

Abbreviations: DAPI, 4′,6-diamidino-2-phenylindole; GFP, green fluorescent protein; NIR, near-infrared; NIR-27, heptamethine indocyanine dye.

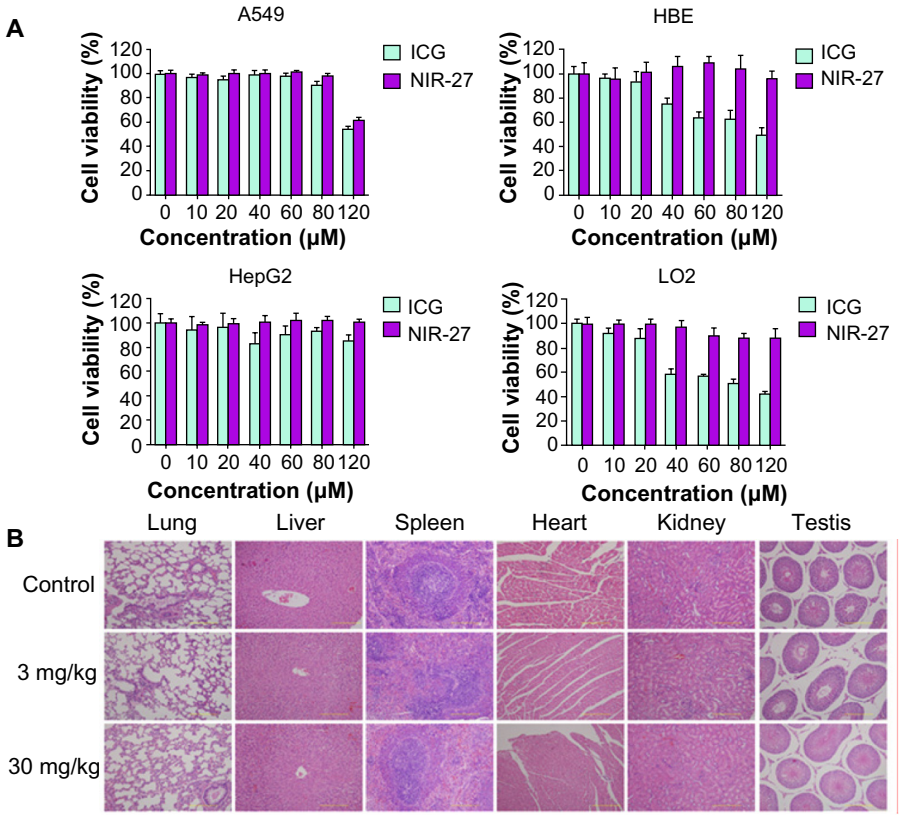

Figure 4 Cytotoxicity assay and acute toxicity of NIR-27 in rats.

Notes: (**A**) The viability of A549, HBE, HepG2, and LO2 cells cultured with NIR-27 in comparison with ICG at the same dose. The data are presented as the mean ± SD (n=6). (**B**) Histological studies on the major organs of the NIR-27 injected mice after 7days.

Abbreviations: HBE, human bronchial epithelial cells; ICG, indocyanine green; NIR-27, heptamethine indocyanine dye; SD, standard deviation.

toxicity of NIR-27 in rats. The effect of NIR-27 on the physical activities and the body weight of the rats was monitored first. There were no animal deaths or symptoms of poisoning. The body weights of the control set and the two experimental sets of rats maintained similar increasing trends for 7 days (see Figure S6). To reveal any potential toxic effect of NIR-27 on the treated rats, blood biochemistry analysis and hematology was carefully performed, including: white blood cell count, red blood cell count, hemoglobin, platelet count, serum alanine aminotransferase, aspartate aminotransferase, alkaline phosphatase, blood urea nitrogen, creatinine, and total cholesterol. There were no statistically significant differences in any of these parameters (see Table S1). These results were also confirmed by the histopathologic analysis of the main organs (lung, liver, spleen, heart, kidney, and testes) dissected from NIR-27-treated rats, which showed no abnormality in comparison to host organs harvested from control rats (Figure 4B).

Conclusion

In summary, we have synthesized a new heptamethine dye (NIR-27) modified with two water-soluble glycine moieties at the end of two N-alkyl side chains. NIR-27 was active in the NIR spectral range and fairly stable in serum. It showed cancer-targeting NIR imaging properties in multiple human tumor xenografts without the necessity of chemical conjugation. Additionally, NIR-27 was demonstrated to have lower cytotoxicity than ICG, and acute toxicity was not observed when its dosage was increased by 100-fold of the imaging dose. These characteristics make NIR-27 a promising prospect as a biocompatible NIR fluorescent sensor for sensitive cancer detection.

Acknowledgments

This work was supported by the State Key Basic Research Development Program (2012CB518103), Natural Science Foundation Programs (81130026 and 81372727), and the Program of New Century Excellent Talents in University (NCET-11-0869) from Ministry of Education and Innovation team building program of Chongqing University (KJTD201338). Qingrong Qi is a co-corresponding author who jointly directed this work.

Disclosure

The authors report no conflicts of interest in this work.

References

1. Fass L. Imaging and cancer: a review. *Mol Oncol*. 2008;2(2):115–152.
2. Hilderbrand SA, Weissleder R. Near-infrared fluorescence: application to in vivo molecular imaging. *Curr Opin Chem Biol*. 2010; 14(1):71–79.
3. Frangioni JV. In vivo near-infrared fluorescence imaging. *Curr Opin Chem Biol*. 2003;7(5):626–634.
4. Caesar J, Shaldon S, Chiandussi L, Guevara L, Sherlock S. The use of indocyanine green in the measurement of hepatic blood flow and as a test of hepatic function. *Clin Sci*. 1961;21:43–57.
5. Benya R, Quintana J, Brundage B. Adverse reactions to indocyanine green: a case report and a review of the literature. *Cathet Cardiovasc Diagn*. 1989;17(4):231–233.
6. Hope-Ross M, Yannuzzi LA, Gragoudas ES, et al. Adverse reactions due to indocyanine green. *Ophthalmology*. 1994;101(3):529–533.
7. Marshall MV, Rasmussen JC, Tan IC, et al. Near-Infrared Fluorescence Imaging in Humans with Indocyanine Green: A Review and Update. *Open Surg Oncol J*. 2010;2(2):12–25.
8. Liu F, Deng D, Chen X, Qian Z, Achilefu S, Gu Y. Folate-polyethylene glycol conjugated near-infrared fluorescence probe with high targeting affinity and sensitivity for in vivo early tumor diagnosis. *Mol Imaging Biol*. 2010;12(6):595–607.
9. Tung CH, Lin Y, Moon WK, Weissleder R. A receptor-targeted near-infrared fluorescence probe for in vivo tumor imaging. *Chembiochem*. 2002;3(8):784–786.
10. Morales AR, Yanez CO, Zhang Y, et al. Small molecule fluorophore and copolymer RGD peptide conjugates for ex vivo two-photon fluorescence tumor vasculature imaging. *Biomaterials*. 2012;33(33):8477–8485.
11. Choi HS, Gibbs SL, Lee JH, et al. Targeted zwitterionic near-infrared fluorophores for improved optical imaging. *Nat Biotechnol*. 2013;31(2):148–153.
12. Chang SK, Rizvi I, Solban N, Hasan T. In vivo optical molecular imaging of vascular endothelial growth factor for monitoring cancer treatment. *Clin Cancer Res*. 2008;14(13):4146–4153.
13. Xu H, Baidoo K, Gunn AJ, et al. Design, synthesis, and characterization of a dual modality positron emission tomography and fluorescence imaging agent for monoclonal antibody tumor-targeted imaging. *J Med Chem*. 2007;50(19):4759–4765.
14. Shen BQ, Xu K, Liu L, et al. Conjugation site modulates the in vivo stability and therapeutic activity of antibody-drug conjugates. *Nat Biotechnol*. 2012;30(2):184–189.
15. Strop P, Liu SH, Dorywalska M, et al. Location matters: site of conjugation modulates stability and pharmacokinetics of antibody drug conjugates. *Chem Biol*. 2013;20(2):161–167.
16. Cheng Z, Al Zaki A, Hui JZ, Muzykantov VR, Tsourkas A. Multifunctional nanoparticles: cost versus benefit of adding targeting and imaging capabilities. *Science*. 2012;338(6109):903–910.
17. Zhang C, Liu T, Su Y, et al. A near-infrared fluorescent heptamethine indocyanine dye with preferential tumor accumulation for in vivo imaging. *Biomaterials*. 2010;31(25):6612–6617.
18. Shi C, Zhang C, Su Y, Cheng T. Cyanine dyes in optical imaging of tumours. *Lancet Oncol*. 2010;11(9):815–816.
19. Tan X, Luo S, Wang D, Su Y, Cheng T, Shi C. A NIR heptamethine dye with intrinsic cancer targeting, imaging and photosensitizing properties. *Biomaterials*. 2012;33(7):2230–2239.
20. Luo S, Zhang E, Su Y, Cheng T, Shi C. A review of NIR dyes in cancer targeting and imaging. *Biomaterials*. 2011;32(29):7127–7138.
21. Mahounga DM, Shan L, Jie C, Du C, Wan S, Gu Y. Synthesis of a novel L-methyl-methionine-ICG-Der-02 fluorescent probe for in vivo near infrared imaging of tumors. *Mol Imaging Biol*. 2012;14(6):699–707.
22. Preston TC, Nuruzzaman M, Jones ND, Mittler S. Role of hydrogen bonding in the pH-dependent aggregation of colloidal gold particles bearing solution-facing carboxylic acid groups. *J Phys Chem C*. 2009;113(32):14236–14244.
23. Luo S, Tan X, Qi Q, et al. A multifunctional heptamethine near-infrared dye for cancer theranosis. *Biomaterials*. 2013;34(9):2244–2251.
24. Zhang C, Wang S, Xiao J, et al. Sentinel lymph node mapping by a near-infrared fluorescent heptamethine dye. *Biomaterials*. 2010;31(7): 1911–1917.
25. Nakayama A, Bianco AC, Zhang CY, Lowell BB, Frangioni JV. Quantitation of brown adipose tissue perfusion in transgenic mice using near-infrared fluorescence imaging. *Mol Imaging*. 2003;2(1):37–49.

26. Andreev OA, Dupuy AD, Segala M, et al. Mechanism and uses of a membrane peptide that targets tumors and other acidic tissues in vivo. *Proc Natl Acad Sci U S A*. 2007;104(19):7893–7898.
27. Velupillai P, Sung CK, Tian Y, et al. Polyoma virus-induced osteosarcomas in inbred strains of mice: host determinants of metastasis. *PLoS Pathog*. 2010;6(1):e1000733.

Supplementary materials

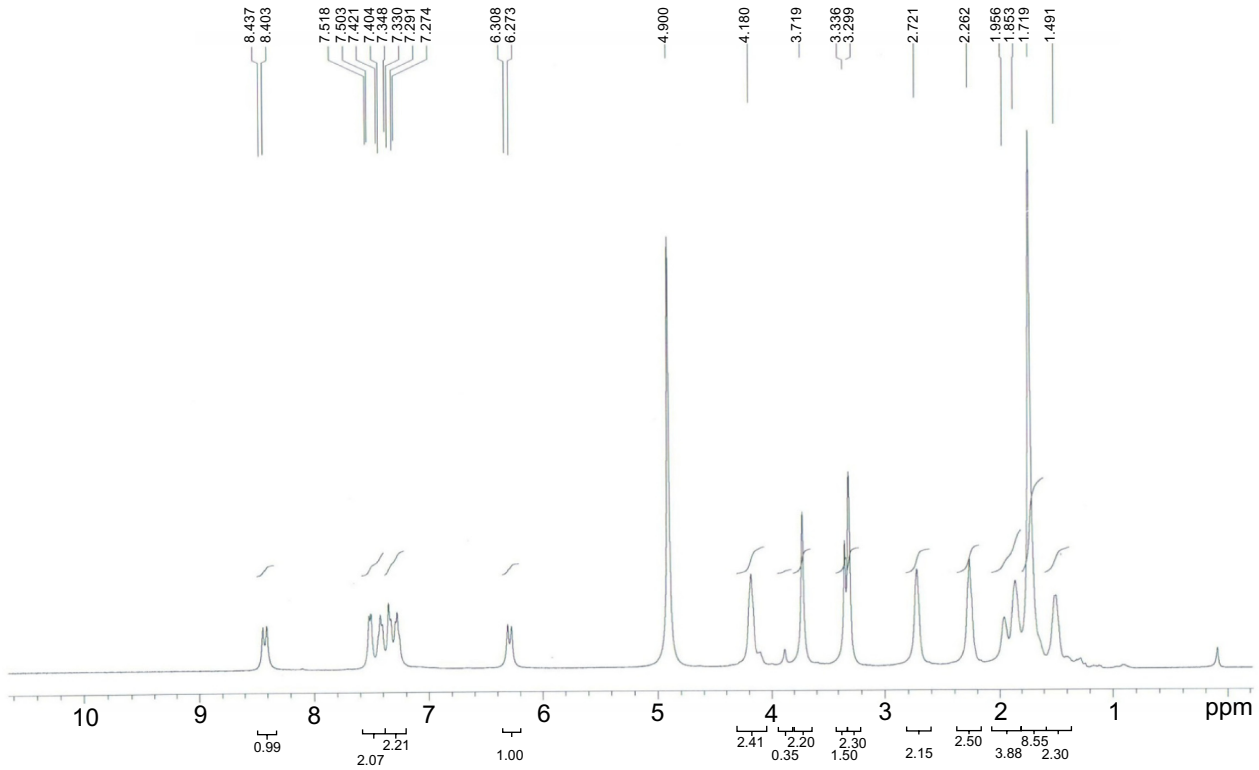

Figure S1 ^{1}H NMR of NIR-27.
Abbreviation: NIR-27, heptamethine indocyanine dye.

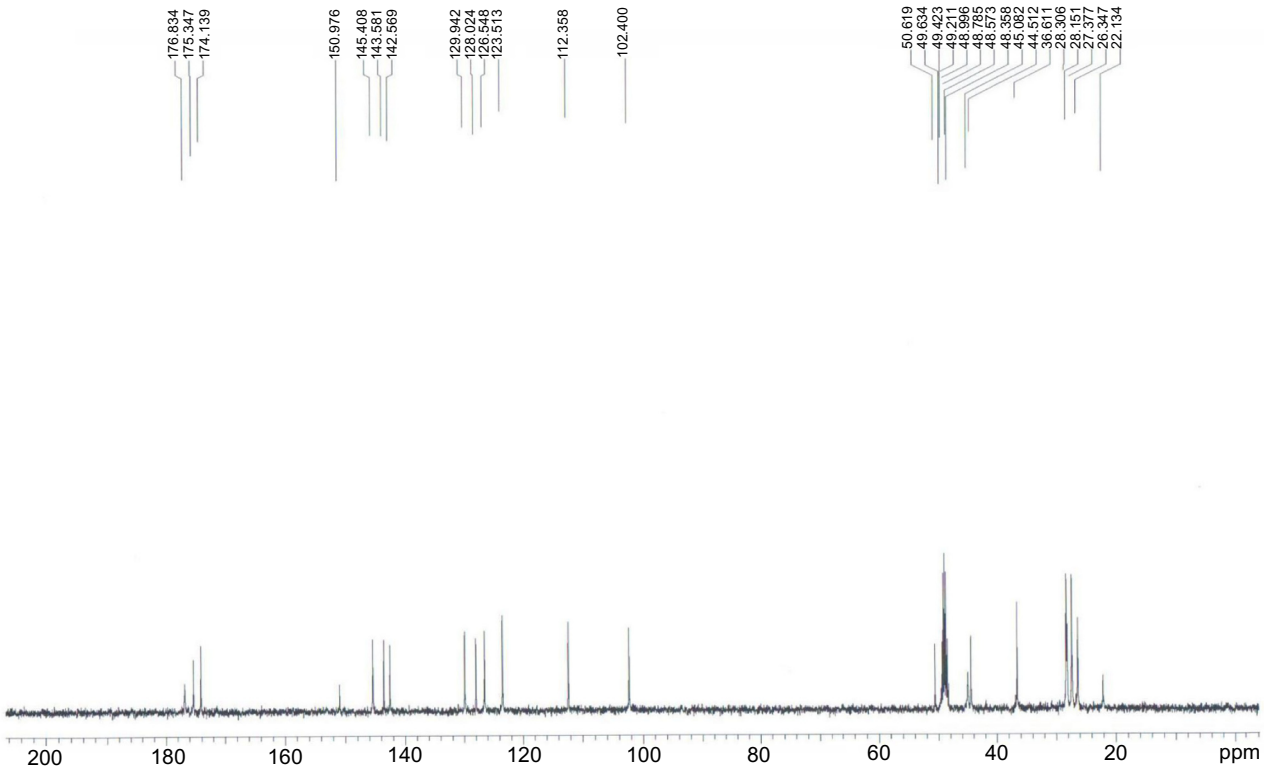

Figure S2 ^{13}C NMR of NIR-27.
Abbreviation: NIR-27, heptamethine indocyanine dye.

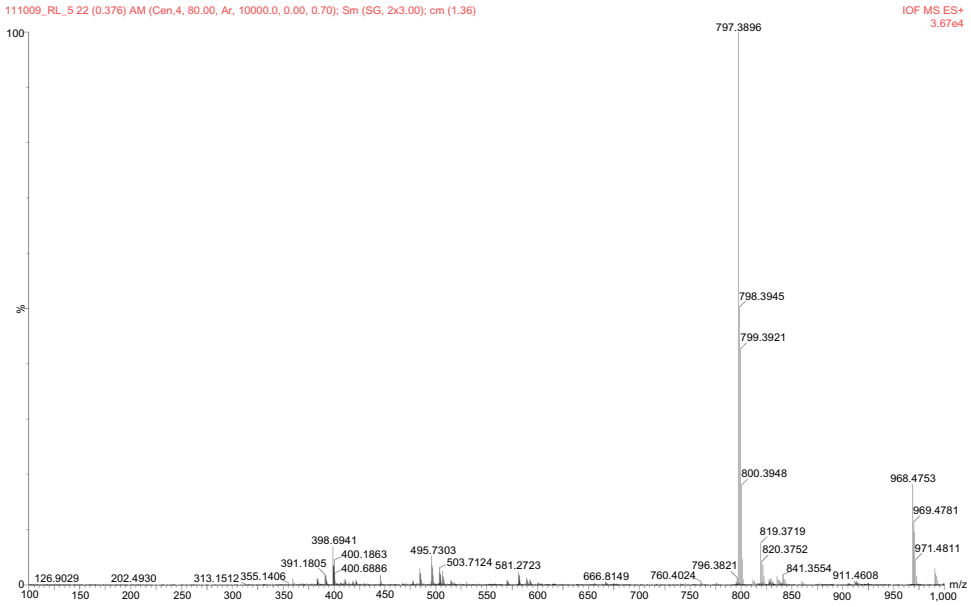

Figure S3 HRMS of NIR-27.
Abbreviations: HRMS, high-resolution mass spectra; NIR-27, heptamethine indocyanine dye.

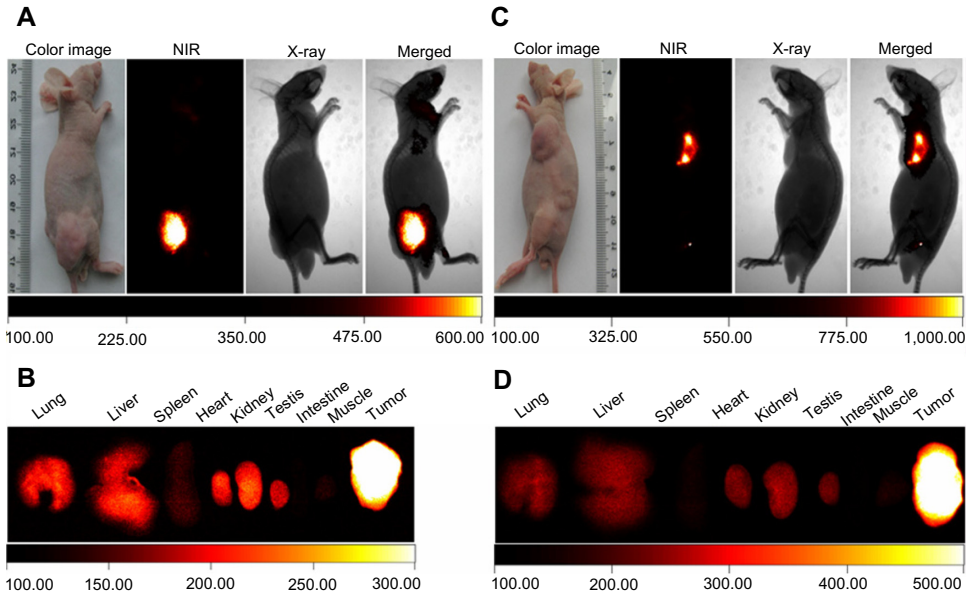

Figure S4 The preferential accumulation of NIR-27 in tumor xenografts.
Notes: Images of the preferential accumulation of NIR-27 in athymic nude mice bearing pre-established human MKN-45 tumor xenografts (**A**) and athymic nude mice with human A549 tumor xenografts (**C**) were shown. All of the animals were successively subjected to NIR imaging and X-ray imaging with the Kodak In-Vivo Imaging System FX Pro after administration of NIR-27 at a dose of 0.3 mg/kg, and the two images were merged for tumor localization. Images showed all the tumors at 72 hours after NIR-27 injection. The fluorescent intensity of dissected organs further confirmed the preferential accumulation of NIR-27 in tumors (**B** and **D**).
Abbreviations: NIR, near-infrared; NIR-27, heptamethine indocyanine dye.

Table S1 Blood physiological and biochemical indexes of rats treated with NIR-27 at the doses of 3 and 30 mg/kg and the control group

Group	WBC ($\times 10^9$/L)	RBC ($\times 10^{12}$/L)	HGB (g/L)	PLT ($\times 10^9$/L)	ALT (IU/L)	AST (IU/L)	ALP (IU/L)	BUN (mmol/L)	Cr (μmol/L)	TCHO (mmol/L)
3 mg/kg	8.88±1.41	4.5±0.1	82±2.65	401.33±181.64	47±1.73	146.33±6.11	463.67±53.72	7.57±0.5	27±1	1.79±0.15
30 mg/kg	6.66±0.15	4.33±0.14	79.67±4.62	417.33±114.29	44.67±1.15	151.67±15.53	401.67±121.63	7.67±0.31	25.67±2.89	1.77±0.08
Control	8.38±1.79	4.7±0.22	89.67±3.79	492±134.64	58±24.98	202.33±43.13	720.33±46.52	7.97±0.57	29±1.73	1.59±0.26

Notes: n=3; All the values are expressed as mean ± standard deviation.
Abbreviations: ALT, alanine aminotransferase; AST, aspartate aminotransferase; BUN, blood urea nitrogen; Cr, creatinine; HGB, hemoglobin; PLT, platelet count; RBC, red blood cell; TCHO, total cholesterol; WBC, white blood cell.

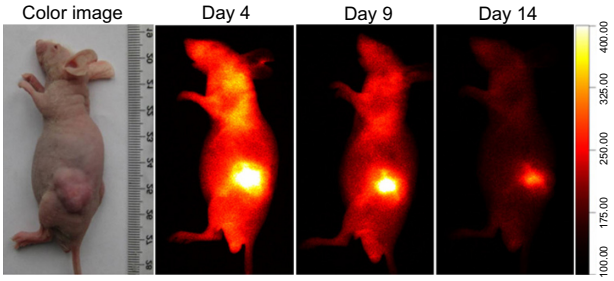

Figure S5 NIR fluorescence images of mice bearing a HL-60 tumor within 14 days after intravenous injection of NIR-27 at a dose of 0.3 mg/kg.
Abbreviations: NIR, near-infrared; NIR-27, heptamethine indocyanine dye.

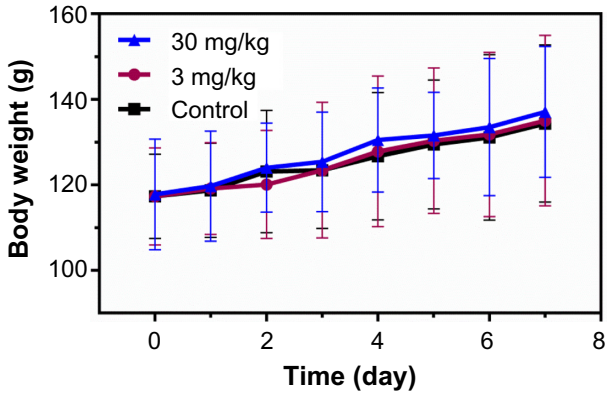

Figure S6 Body weight changes of the male rats treated with NIR-27 at the dose of 3 and 30 mg/kg (corresponding to 10- and 100-fold of the imaging dose) through tail vein at different time points.
Notes: Age-matched rats were intravenously injected with saline as the control set. Error bars were based on standard deviations of three rats per group.
Abbreviation: NIR-27, heptamethine indocyanine dye.

Drug Design, Development and Therapy

Dovepress

Publish your work in this journal

Drug Design, Development and Therapy is an international, peer-reviewed open-access journal that spans the spectrum of drug design and development through to clinical applications. Clinical outcomes, patient safety, and programs for the development and effective, safe, and sustained use of medicines are a feature of the journal, which has also been accepted for indexing on PubMed Central. The manuscript management system is completely online and includes a very quick and fair peer-review system, which is all easy to use. Visit http://www.dovepress.com/testimonials.php to read real quotes from published authors.

Submit your manuscript here: http://www.dovepress.com/drug-design-development-and-therapy-journal